

Approximate analytic solutions of adiabatic capillary tube

Chunlu Zhang*, Guoliang Ding

Institute of Refrigeration and Cryogenics, Shanghai Jiaotong University, Shanghai 200030, China

Received 8 October 2002; received in revised form 5 June 2003; accepted 17 July 2003

Abstract

Approximate analytic solution of capillary tube is valuable for theoretical analysis and engineering calculation. In this work, two kinds of approximate analytic solutions of adiabatic capillary tube have been developed. One is the explicit function of capillary tube length. Another is the explicit function of refrigerant mass flow rate. In these solutions, the choked flow condition is taken into account without iterative calculations. The approximate predictions are found to agree reasonably well with experimental data in open literatures.

© 2003 Elsevier Ltd and IIR. All rights reserved.

Keywords: Capillary tube; Calculation; Expansion; Refrigerant; Flow; Adiabatic

Tube capillaire adiabatique : analyses approximatives

Mots clés : Capillaire ; Calcul ; Détente ; Frigorigène ; Débit ; Adiabatique

1. Introduction

The capillary tube is widely used as a throttling device in the small-scale vapor-compression refrigeration equipment such as room air conditioners, household refrigerators and freezers. It is simple, reliable and inexpensive. A number of research works have been carried out since 1940 both in theory and experiment [1–3]. Especially in the past 15 years or so, the capillary characteristics have been widely studied with alternative refrigerants.

Numerical modelling and correlation play an important role in the design of capillary tubes. The distributed-parameter model is the most popular model used by the researchers because it is of the general mechanism and acceptable precision [4–10]. However,

the computation of the distributed-parameter model is somewhat time-consuming and its program skills are not easy for most engineers. It has therefore not been widely used in engineering design. In contrast, the empirical correlations are simple to calculate and practicable for engineering purposes. However, they are available only in the range of regressive data and cannot be arbitrarily extrapolated [10–14]. To balance the generalization and simplicity of the above two types of models, a novel approximate analytical approach was first developed by Yilmaz and Ünal [15]. Their work is valuable to simplify the distributed-parameter model of an adiabatic capillary tube. In their work, however, the reference point was not appropriately chosen and the choked flow condition at the exit of the capillary tube was not considered. This could lead to incorrect results or failure in calculation. Zhang and Ding [16] analyzed the existing problems in Yilmaz and Ünal's work and gave some modifications. The modified model could be in good agreement with the distributed-parameter one.

* Corresponding author. Tel.: +86-21-6293-2110; fax: +86-21-6293-2601.

E-mail address: clzhang@sjtu.edu.cn (C.L. Zhang).

Nomenclature

C_1, C_2	empirical constants, defined in Eq. (19)
D	inner diameter (m)
F	friction factor
G	mass flux ($\text{kg s}^{-1} \text{m}^{-2}$)
H	enthalpy (J kg^{-1})
L	capillary tube length (m)
M	mass flow rate (kg s^{-1})
P	pressure (Pa)
Re	Reynolds number
T	temperature ($^{\circ}\text{C}$)
v	specific volume ($\text{m}^3 \text{kg}^{-1}$)
X	quality

Greek letters

β	slope of Eq. (4)
μ	viscosity ($\text{kg m}^{-1} \text{s}^{-1}$)
π	the ratio of the circumference of a circle to its diameter ($= 3.14159 \dots$)

Superscripts and Subscripts

*	dimensionless parameter
3	point 3 in Fig. 1
ch	choked or critical condition
e	evaporating
f	saturated liquid
g	saturated vapor
in	inlet
liq	liquid region
out	outlet
pre	predictor
r	reference point
tp	two-phase region

However, the consideration of the choked flow condition caused the iterative calculation. Therefore, the approximate analytic model is not an explicit solution yet and had better be transformed into some explicit functions of the refrigerant mass flow rate or the capillary tube length.

In this work, the explicit approximate analytic solution of the refrigerant mass flow rate through an adiabatic capillary tube or that of the capillary tube length for the desired mass flow rate have been developed on the basis of the previous work [15,16].

2. Brief of previous work

In engineering, the flow in adiabatic capillary tubes can be treated as a homogeneous equilibrium flow [16]. Although the mass flow rate of adiabatic capillary tubes

will be underestimated if the effect of underpressure of evaporation is not considered, the quantification method is not mature and the deviation of underestimation is not obvious [7,16]. Therefore, it was not considered in the previous work [15,16], nor in this work.

The governing equations are as follows:

$$\frac{dG}{dL} = 0 \quad (1)$$

$$\frac{d(h + \frac{1}{2}G^2v^2)}{dL} = 0 \quad (2)$$

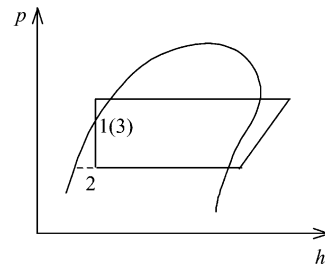
$$-dp = G^2dv + \frac{f}{2D}G^2vdL \quad (3)$$

Here, are G the mass flux, p the pressure, v the specific volume, h the specific enthalpy, f the friction factor, D the inner diameter, L the length of the capillary tube.

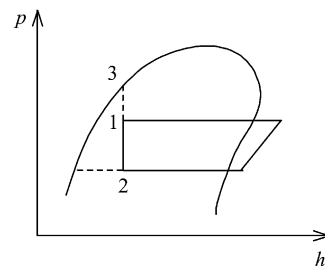
Yilmaz and Ünal [15] assumed that the process in capillary tube is isenthalpic. It is a good approximation of the adiabatic process in capillary tube. Based on the Clausius–Clapeyron equation, Yilmaz and Ünal established the following approximate relation between v and p in two-phase region.

$$v^* = 1 + \beta(1/p^* - 1) \quad (4)$$

where, $p^* = p/p_r, v^* = v/v_r$. Subscript r stands for the reference point. The reference point was defined as the crossing point of the isenthalpic line and the saturated liquid line in the pressure–enthalpy diagram, namely



(a) subcooled inlet in throttling process



(b) two-phase inlet in throttling process

Fig. 1. Schematic of throttling process.

point 3 in Fig. 1. The slope of Eq. (4), β was evaluated by

$$\beta = 2.62 \times 10^5 / p_3^{0.75} \quad (5)$$

where, p_3 is the pressure at point 3.

As shown in Fig. 2, linearity of Eq. (4) is fairly good. Yilmaz and Ünal [15] showed the good linearity for some pure refrigerants. The authors tested it for more refrigerants and refrigerant mixtures and found it is available for refrigerant mixtures, too. For the purpose of perspicuity, only part of them is shown in Fig. 2.

The mean slope of each line similar to those in Fig. 2 is calculated under different operating conditions and plotted in Fig. 3. It can be found that Eq. (5) is a good correlation for not only refrigerants but also refrigerant mixtures. Since the refrigerant mixtures were not considered by Yilmaz and Ünal [15], they can be regarded as the independent verification. A better correlation presented by the authors is as follows.

$$\beta = 1.63 \times 10^5 / p_3^{0.72} \quad (6)$$

The slight difference between Eqs. (5) and (6) might be caused by the calculation of refrigerant thermodynamic properties. Different from Yilmaz and Ünal [15], the authors use the well-known REFPROP 6.01 [17] in this work.

Zhang and Ding [16] redefined the reference point as the start point of two-phase region, namely point 1 in Fig. 1. Correspondingly, The slope of Eq. (4), β can be updated as

$$\beta = \frac{(1.63 \times 10^5 / p_3^{0.72}) p_3^*}{1 + (1.63 \times 10^5 / p_3^{0.72}) (p_3^* - 1)} \quad (7)$$

For the subcooled inlet, as shown in Fig. 1(a), the redefined reference point is the same as that defined by Yilmaz and Ünal [15] and Eq. (7) will reduce to Eq. (6). For the two-phase inlet, as shown in Fig. 1(b), the start

point of two-phase region is not the saturated liquid point any longer.

Substituting Eq. (4) into Eq. (3) and taking integral, one obtains the length of two-phase region.

$$L_{tp} = \frac{2D}{f_{tp}} \ln \left(\frac{p_{out}^*}{\beta + (1 - \beta)p_{out}^*} \right) - \frac{2D}{f_{tp} G^{*2} (1 - \beta)} \times \left\{ p_{out}^* - 1 - \frac{\beta}{1 - \beta} \ln [\beta + (1 - \beta)p_{out}^*] \right\}, \quad (8)$$

where, dimensionless mass flux

$$G^* = G \sqrt{v_r / p_r}. \quad (9)$$

In addition, the length of liquid region can be written as

$$L_{liq} = \frac{2D(p_{in} - p_r)}{f_{in} G^2 v_{in}} = \frac{2D(p_{in}^* - 1)}{f_{in} G^{*2}}. \quad (10)$$

Consequently, the length of a capillary tube is

$$L = \frac{2D(p_{in}^* - 1)}{f_{in} G^{*2}} + \frac{2D}{f_{tp}} \ln \left(\frac{p_{out}^*}{\beta + (1 - \beta)p_{out}^*} \right) - \frac{2D}{f_{tp} G^{*2} (1 - \beta)} \times \left\{ p_{out}^* - 1 - \frac{\beta}{1 - \beta} \ln [\beta + (1 - \beta)p_{out}^*] \right\}. \quad (11)$$

Eq. (11) is the explicit approximate solution of capillary tube length when the flow is not choked. Yilmaz and Ünal [15] did not take the choked flow condition into account. It could lead to abnormal results in calculation. Zhang and Ding [16] considered this case by using the critical mass flux as the maximum local mass flux. Unfortunately, it was not explicit expression any more and the iterative calculation was needed in their work.

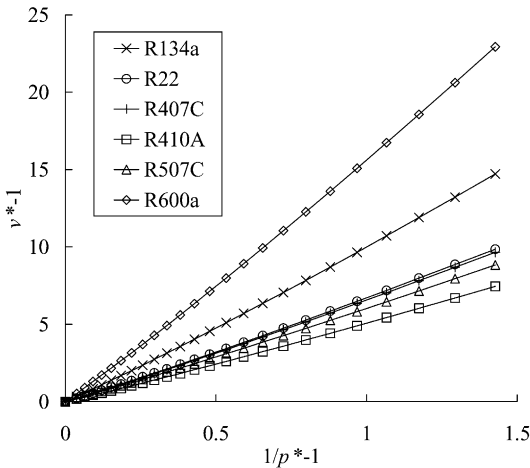


Fig. 2. Illustration of Eq. (4).

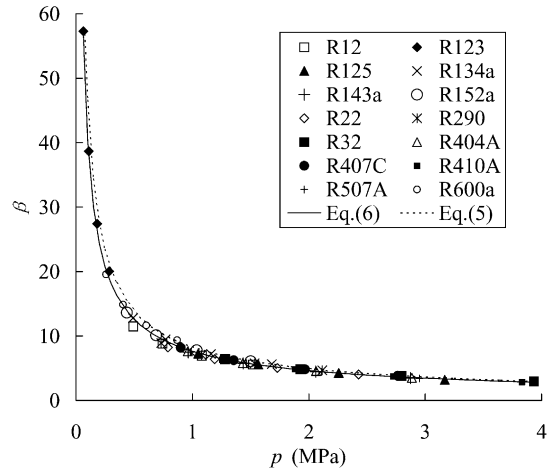


Fig. 3. Illustration of Eqs. (5) and (6).

All in all, a complete explicit approximate solution of capillary tube length has not been developed. In addition, because Eq. (11) is a complicated implicit function of mass flow rate, it cannot be directly transformed into an explicit expression of mass flow rate.

3. Approximate solution of tube length (L-solution)

According to the above-mentioned previous work, one can evaluate the approximate length of an adiabatic capillary tube when the flow is not choked. As for the choked flow condition, a new evaluation method different from Zhang and Ding [16] are introduced here. It has been proved by Chung [8].

$$\frac{dL}{dp} \leq 0 \quad (12)$$

where, if and only if the flow is choked, the equality will be reached.

In other words, for a given mass flow rate the length of a capillary tube will increase with descent of the evaporating pressure (or the back pressure). When the evaporating pressure lowers to the choked pressure, the tube length will reach the maximum. Lowering the evaporating pressure below the choked pressure will not result in an increase in the capillary tube length. Namely,

$$\frac{dL}{dp_{out}} \leq 0 \quad (13)$$

Applying Eq. (13) to Eq. (11), we have

$$p_{out}^* \geq \sqrt{\beta G^*} \quad (14)$$

Therefore when the flow through the capillary tube is choked, the reduced choked pressure at the exit plane is

$$p_{ch}^* = \sqrt{\beta G^*} \quad (15)$$

If the exit pressure evaluated by Eq. (15) is higher than the evaporating pressure, the flow through the capillary tube will be choked. Substituting Eq. (15) into Eq. (11), one can obtain the length of the adiabatic capillary tube under the choked flow condition.

$$L = \frac{2D(p_{in}^* - 1)}{f_{in} G^*} + \frac{2D}{f_{tp}} \ln \left(\frac{\sqrt{\beta G^*}}{\beta + (1 - \beta)\sqrt{\beta G^*}} \right) - \frac{2D}{f_{tp} G^* (1 - \beta)} \left\{ \sqrt{\beta G^*} - 1 - \frac{\beta}{1 - \beta} \ln \left[\beta + (1 - \beta)\sqrt{\beta G^*} \right] \right\} \quad (16)$$

In Eqs. (11) and (16), the friction factor, especially the two-phase friction factor, is an important factor in calculation. In general, the friction factor of capillary tube is weakly dependent on the roughness [5] and can be evaluated by some relation as follows [7,10].

$$f = C_1 \text{Re}^{-C_2} = C_1 \left(\frac{GD}{\mu} \right)^{-C_2} \quad (17)$$

where, C_1 and C_2 are empirical constants. Bittle and Pate [7] recommended $C_1 = 0.23$ and $C_2 = 0.216$.

In two-phase region, the viscosity in Eq. (17) is calculated by the McAdams model [18] that was recommended by Bittle and Pate [7].

$$\frac{1}{\mu_{tp}} = \frac{x}{\mu_g} + \frac{1-x}{\mu_f} \quad (18)$$

Fig. 4 gives the distribution of two-phase friction factor under a typical operating condition of adiabatic capillary tube (I.D. 1 mm, length 1 m, saturated liquid inlet at the temperature 45 °C). For the purpose of perspicuity, only part of refrigerants has been shown in Fig. 4. It shows that the maximum difference of two-phase friction factor between inlet and outlet of two-phase region is about 10%. It means that the average two-phase friction factor is about 5% below the inlet value. The small variation of friction factor in two-phase region can be explained with Eq. (17). The two-phase friction factor varies with the viscosity. However, the variation of the two-phase viscosity is strongly weakened by the small exponent C_2 . Therefore, It is acceptable in engineering to use the friction factor at the entrance of two-phase region instead of the average two-phase friction factor.

Summing up the above results, the flow chart of sizing the capillary tube length is shown in Fig. 5. There is no iteration in judgment and calculation of the choked flow condition.

4. Approximate solution of mass flow rate (M-solution)

According to the L-solution, one can find that the tube length is a complicated function of the mass flux and other parameters. It is hard to directly derive an explicit expression of the mass flow rate from the complicated function. Therefore, we use a predictor-corrector approach to the M-solution. At first, a predictor solution is obtained from simplification of the L-solution. Then a corrector solution is found on the basis of the predictor solution.

4.1. M-predictor solution

Concerning the choked flow condition, we consider the following approximate relation.

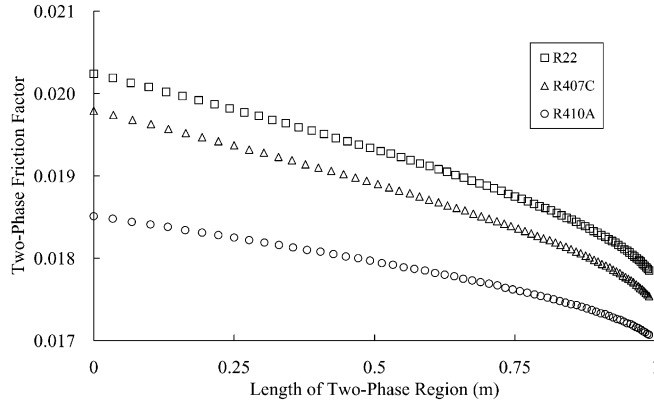


Fig. 4. Distribution of friction factor in two-phase region.

$$\ln(1+z) \approx z, \quad |z| < 1. \quad (19)$$

When the absolute value of z is far less than 1, Eq. (19) will be of high precision. Let

$$z = \frac{1-\beta}{\beta} \sqrt{\beta} G^*. \quad (20)$$

Considering Eq. (15) and the fact that $\beta > 1$, we have

$$|z| = \frac{\beta-1}{\beta} \sqrt{\beta} G^* = \frac{\beta-1}{\beta} p_{ch}^* < p_{ch}^*.$$

Normally, $p_{ch}^* = 0.3 \sim 0.5$. Therefore, Eq. (19) is an acceptable approximation to predictor solution when

variable z is defined by Eq. (20). Substituting Eqs. (19) and (20) into Eq. (16), one has

$$L = \frac{2D(p_{in}^* - 1)}{f_{in} G^{*2}} + \frac{2D}{f_{tp}} \left(\frac{\beta-1}{\sqrt{\beta}} G^* + \ln G^* - \frac{\ln \beta}{2} \right) + \frac{2D[1 + \beta(\ln \beta - 1)]}{f_{tp} G^{*2} (1-\beta)^2} \quad (21)$$

Comparing the three items on the right side of Eq. (21), we find that the second item is a small quantity relative to other two items because $G^* \ll 1$ under typical operating conditions. Hence the second item can be omitted and Eq. (21) is further reduced as

$$L = \frac{2D(p_{in}^* - 1)}{f_{in} G^{*2}} + \frac{2D[1 + \beta(\ln \beta - 1)]}{f_{tp} G^{*2} (1-\beta)^2}. \quad (22)$$

Substituting Eq. (17) into Eq. (22) and using f_{in} instead of f_{tp} , we obtain the mass flow rate under the choked condition.

$$m_p = \frac{\pi D^2}{4} \times \left\{ \frac{2}{C_1} \left(\frac{D^{1+C_2}}{L} \right) \left(\frac{p_r}{\nu_r \mu_{in}^{C_2}} \right) \left[p_{in}^* - 1 + \frac{1 + \beta(\ln \beta - 1)}{(1-\beta)^2} \right] \right\}^{\frac{1}{2-C_2}} \quad (23)$$

Similar treatment can be applied to the non-choked flow condition. Eq. (11) is reduced as

$$L = \frac{2D(p_{in}^* - 1)}{f_{in} G^{*2}} - \frac{2D}{f_{tp} G^{*2} (1-\beta)} \times \left\{ p_{out}^* - 1 - \frac{\beta}{1-\beta} \ln[\beta + (1-\beta)p_{out}^*] \right\} \quad (24)$$

Substituting Eq. (17) into Eq. (24) and using f_{in} instead of f_{tp} , we have

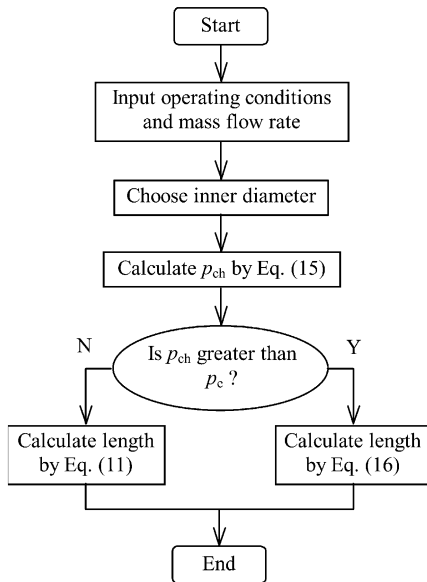


Fig. 5. Flow chart of sizing capillary tube length.

$$m_p = \frac{\pi D^2}{4} \left\{ \frac{2}{C_1} \left(\frac{D^{1+C_2}}{L} \right) \left(\frac{p_r}{v_r \mu_{in}^{C_2}} \right) \left[p_{in}^* - 1 - \left(\frac{p_{out}^* - 1}{1 - \beta} - \frac{\beta}{(1 - \beta)^2} \ln[\beta + (1 - \beta)p_{out}^*] \right) \right] \right\}^{\frac{1}{2-C_2}} \quad (25)$$

Summing up the above results, the flow chart of calculating mass flow rate through a capillary tube with the M-predictor solution is shown in Fig. 6. No iteration is needed in calculation.

4.2. M-corrector solution

The accuracy of the M-predictor solution might be weakened by the above-mentioned approximation. Based on the M-predictor solution, however, a more accurate solution will be obtained when we apply the M-predictor solution to the L-solution.

Concerning the choked flow condition, we substitute the predicted results from Eq. (23) into Eq. (16) and obtain

$$L = \frac{2D(p_{in}^* - 1)}{f_{in,p} G^{*2}} + \frac{2D}{f_{tp,p}} \ln \left(\frac{\sqrt{\beta} G_p^*}{\beta + (1 - \beta)\sqrt{\beta} G_p^*} \right) - \frac{2D}{f_{tp,p} G^{*2}(1 - \beta)} \left\{ \sqrt{\beta} G_p^* - 1 - \frac{\beta}{1 - \beta} \ln[\beta + (1 - \beta)\sqrt{\beta} G_p^*] \right\} \quad (26)$$

$$m = \frac{\pi D^2}{4} \sqrt{\frac{(p_{in}^* - 1) - \frac{f_{in,p}}{f_{tp,p}} \left\{ \frac{\sqrt{\beta} G_p^* - 1}{1 - \beta} - \frac{\beta}{(1 - \beta)^2} \ln[\beta + (1 - \beta)\sqrt{\beta} G_p^*] \right\}}{\frac{L f_{in,p}}{2D} - \frac{f_{in,p}}{f_{tp,p}} \ln \left(\frac{\sqrt{\beta} G_p^*}{\beta + (1 - \beta)\sqrt{\beta} G_p^*} \right)}}} \left(\frac{p_r}{v_r} \right) \quad (27)$$

Similarly, we can deal with the non-choked flow condition and obtain

$$m = \frac{\pi D^2}{4} \sqrt{\frac{(p_{in}^* - 1) - \frac{f_{in,p}}{f_{tp,p}} \left\{ \frac{p_{out}^* - 1}{1 - \beta} - \frac{\beta}{(1 - \beta)^2} \ln[\beta + (1 - \beta)p_{out}^*] \right\}}{\frac{L f_{in,p}}{2D} - \frac{f_{in,p}}{f_{tp,p}} \ln \left(\frac{p_{out}^*}{\beta + (1 - \beta)p_{out}^*} \right)}}} \left(\frac{p_r}{v_r} \right) \quad (28)$$

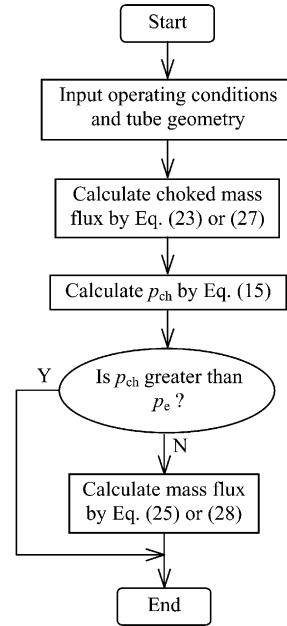


Fig. 6. Flow chart of calculating mass flow rate through a capillary tube.

In the above M-corrector solution, the average friction factor in two-phase region can be estimated by either the inlet value of two-phase region or the average value of inlet and outlet from the M-predictor solution.

The flow chart of calculating mass flow rate through a capillary tube with the M-corrector solution is similar to that with the M-predictor solution, as shown in Fig. 6. Although the M-predictor solution is necessary for running the M-corrector solution, no iteration is needed in calculation yet.

5. Verification

To verify the above-mentioned L-solution and M-solution of adiabatic capillary tubes, experimental data in open literature [4,13,19–23] are used for case study.

In calculation, the average friction factor of two-phase region is needed. As mentioned above, we can choose either the value at the entrance of two-phase region or the modified one with a predictor-corrector method. The mass flow rate is not sensitive to the choice.

Deviations of measured mass flow rates from predictions are shown in Figs. 7–9.

Fig. 7 shows the comparison between the measured mass flow rates and the predictions with the L-solution. Absolute majority of data are within ±15%. As a whole, the predictions are about 5% lower than the measured values. It could be caused by neglecting the effect of underpressure of evaporation. If one needs to

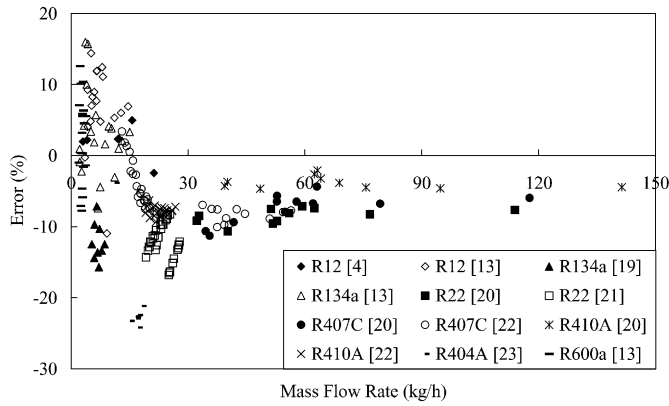


Fig. 7. Deviation of measured mass flow rates from predictions with L-solution.

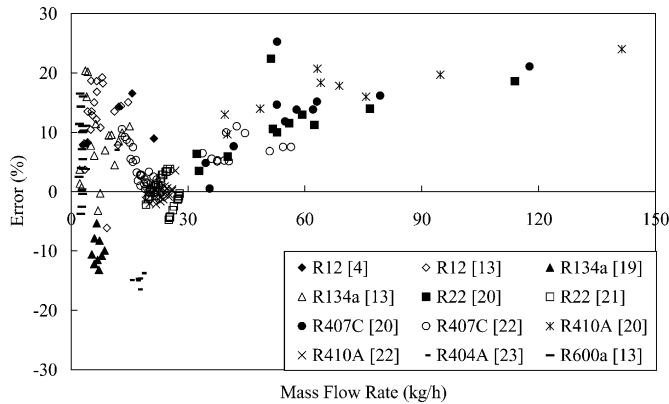


Fig. 9. Deviation of measured mass flow rates from predictions with M-corrector solution.

add the underpressure of evaporation to the above-mentioned solutions, one can easily do it with an additional pressure drop in liquid region. It will not increase the complexity of these solutions.

Fig. 8 shows the comparison between the measured mass flow rates and the predictions with the M-pre-

dictor solution. Most of data fall into -10% – 20% . The M-predictor solution gives a higher prediction than the L-solution because some simplifications are applied from the L-solution to the M-predictor solution. Especially, the omitted items from Eq. (21) to Eq. (22) and from Eq. (11) to Eq. (24) are negative and lead to higher

values in the M-predictor solution. In addition, the approximation of Eq. (19) will go worse if absolute value of z is not small enough. Since the value of z will increase with the mass flux, as seen in Eq. (20), the deviation between the L-solution and the M-predictor solution is larger under the large mass flux than that under the small mass flux.

Fig. 9 shows the comparison between the measured mass flow rates and the predictions with the M-corrector solution. The distribution of deviation is very close to that in Fig. 7. It means that the M-corrector solution is highly consistent with the L-solution, although its predictor solution is not satisfactory under the large mass flux.

From the above-mentioned comparisons, one can see that the present approximate solutions yield good predictions to the experimental data. The deviations are within ± 15 percent for absolute majority of data. It agrees with other models developed by different researchers and may be considered reasonable and satisfactory on account of the simplicity of the present method.

6. Conclusions

Approximate analytic solutions of adiabatic capillary tube are developed in this paper. The L-solution can be used to size the capillary tube with desired mass flow rate. The M-solution can predict the mass flow rate of a given capillary tube. All the solutions are explicit expressions for the choked and non-choked flow conditions. Compared with the distributed-parameter models, the approximate analytic solutions are simple and free of iterative calculation. Consequently, they are very easy and fast in calculation. On the other hand, compared with the empirical correlations, the approximate analytic solutions are of better generalization. In addition, the comparisons between the present solutions and the experimental data in open literature are also satisfactory.

References

- [1] ASHRAE. ASHRAE handbook—refrigeration. Atlanta, CA: American Society of Heating, Refrigerating and Air-Conditioning Engineers, Inc., 1998; chapter 45.
- [2] Schulz UW. State of the art: the capillary tube for, and in, vapor compression systems. ASHRAE Transactions 1985; 91(1):92–105.
- [3] Fang XD. Flow calculations for fixed-area expansion devices. ASHRAE Transactions 2001;107(1):130–9.
- [4] Li RY, Lin S, Chen ZH. Numerical modeling of thermodynamic non-equilibrium flow of refrigerant through capillary tubes. ASHRAE Transactions 1990;96(1):542–9.
- [5] Kuehl SJ, Goldschmidt VW. Modeling of steady flows of R-22 through capillary tubes. ASHRAE Transactions 1991;97(1):139–48.
- [6] Escanes F, Perez-Segarra CD, Oliva A. Numerical simulation of capillary-tube expansion devices. Int J Refrig 1995;18(2):113–22.
- [7] Bittle RR, Pate MB. A theoretical model for predicting adiabatic capillary tube performance with alternative refrigerants. ASHRAE Transactions 1996;102(2): 52–64.
- [8] Chung M. A numerical procedure for simulation of Fanno flows of refrigerants or refrigerant mixtures in capillary tubes. ASHRAE Transactions 1998;104(2):1031–42.
- [9] Garcia-Valladares O, Perez-Segarra CD, Oliva A. Numerical simulation of capillary tube expansion devices behavior with pure and mixed refrigerants considering metastable region. Part I: mathematical formulation and numerical model. Applied Thermal Engineering 2002; 22(2):173–82.
- [10] Jung D, Park C, Park B. Capillary tube selection for HCFC22 alternatives. Int J Refrig 1999;22(8):604–14.
- [11] Bansal PK, Rupasinghe AS. An empirical model for sizing capillary tubes. Int J Refrig 1996;19(8):497–505.
- [12] Bittle RR, Wolf DA, Pate MB. A generalized performance prediction method for adiabatic capillary tubes. HVAC&R Research 1998;4(1):27–43.
- [13] Melo C, Ferreira RTS, Neto CB, Goncalves JM, Mezavila MM. An experimental analysis of adiabatic capillary tubes. Applied Thermal Engineering 1999;19(6):669–84.
- [14] Chen SL, Liu CH, Cheng CS, Jwo CS. Simulation of refrigerants flowing through adiabatic capillary tubes. HVAC&R Research 2000;6(2):101–15.
- [15] Yilmaz T, Ünal S. General equation for the design of capillary tubes. ASME Journal of Fluids Engineering 1996;118(2):150–4.
- [16] Zhang CL, Ding GL. Modified general equation for the design of capillary tubes. ASME Journal of Fluids Engineering 2001;123(4):914–9.
- [17] McLinden MO, Klein SA, Lemmon EW, Peskin AP. NIST thermodynamic and transport properties of refrigerants and refrigerant mixtures (REFPROP), Version 6.01. Gaithersburg, MD: National Institute of Standards and Technology; 1998.
- [18] McAdams WH, Wood WK, Bryan RL. Vaporization inside horizontal tubes-ii-benzene-oil mixtures. Transactions of the ASME 1942;64:193.
- [19] Wijaya H. Adiabatic capillary tube test data for HFC-134a. Proc. West Lafayette IN: The IIR-Purdue Refrigeration Conference; 1992.
- [20] Kim SG, Kim MS, Ro ST. Experimental investigation of the performance of R22, R407C and R410A in several capillary tubes for air-conditioners. Int J Refrig 2002;25: 521–31.
- [21] Wei CZ, Lin YT, Wang CC, Leu JS. Experimental study of the performance of capillary tubes for R-407C refrigerant. ASHRAE Transactions 1999;105(2):634–8.
- [22] Fiorelli FAS, Huerta AAS, Silveiras OM. Experimental analysis of refrigerant mixtures flow through adiabatic capillary tubes. Experimental Thermal and Fluid Science 2002;26:499–512.
- [23] Yana Motta SF, Parise JAR, Braga SL. A visual study of R-404A/oil flow through adiabatic capillary tubes. Int J Refrig 2002;25:586–96.